Optica Applicata, Vol. XLI, No. 1, 2011

Development of wide range displacement sensors based on polarized light detecting technology

XIAOPING LU*, WEI LI, YONGGANG LIN

The State Key Laboratory of Fluid Power Transmission and Control, Zhejiang University, Hangzhou 310027, China

*Corresponding author: qgb@zju.edu.cn

A series of novel wide range displacement sensors based on polarized light detecting technology is presented. The sensors include a displacement-current comparator and a servo comparison displacement sensor. Special structures and technologies are introduced to the sensor systems to solve the optical problems, such as the nonlinearity, the light source drift *etc*., and realize wide range measurement. The designing, assembling, and testing results of the prototypes of sensors are described. The testing results of the prototypes show that the novel sensors based on polarized light detecting technology have good linearity, and wide range measuring ability.

Keywords: displacement sensor, Malus law, Faraday optical rotation, wide range measurement, optical nonlinearity, light source drift.

1. Introduction

Displacement measurement is one of the basic measurement techniques, and displacement sensors are commonly used in various technology and industrial fields [1]. There exist many angular or rectilinear displacement measuring tasks with a wide range, up to tens of meters, in cases such as a robot, hydraulic executor, rectilinear motor and so on, but just a few displacement sensors can be used to wide range non-contact measurement. Many new technologies have been applied in displacement measuring technology to achieve wide range measurement with high accuracy and low cost [2–4].

Malus law has been used in physical measurements, such as electric or magnetic field intensity, electric current or voltage, temperature, linear acceleration, angular and linear velocities, force, torque, pressure, *etc*. [5–12]. A novel linear displacement sensor was presented by VILLAVERDE *et al*. in 1998 [13]. In the same year, WEI LI from China presented the detailed schematic of a novel displacement sensor with a wide range, based on polarized light detecting technology [14]. A compact sensor adopting

a magnetic garnet crystal working in a saturation state to overcome the temperature drift of the Verdet constant was presented by LI *et al*. in 2005 [15]. And a novel absolute displacement sensor based on Malus law was developed in 2009 [16].

Based on the above research, a series of sensors based on polarizing light detecting technology are proposed. Some special structures and technologies, such as dual light paths with one light source, servo tracking technology, are introduced to eliminate the optical nonlinearity, the light intensity drift, and to realize wide range measurement. The paper describes the concepts and configurations of the sensors, and gives the testing results of the prototypes.

2. Theoretical basis

2.1. Malus law

In a polarized light detection system shown in Fig. 1, according to optical Malus law, we have

$$I = I_0 \cos^2 \theta \tag{1}$$

where I_0 is the light intensity eradiating from a light source and passing through a polarizer, I is the light intensity detected by an analyzer, and θ is the angle between two polarization axes of the polarizer and the analyzer [17].

2.2. Faraday optical rotation

When the polarized light passes through a Faraday rotator in the magnetic field, its polarization plane will be rotated; this phenomenon is Faraday optical rotation

$$\theta = \rho L B \tag{2}$$

where θ is the Faraday optical rotation angle, ρ is the Verdet constant which is only related to the rotation medium; L is the length of the Faraday rotator, B is the intensity of magnetic field [18].

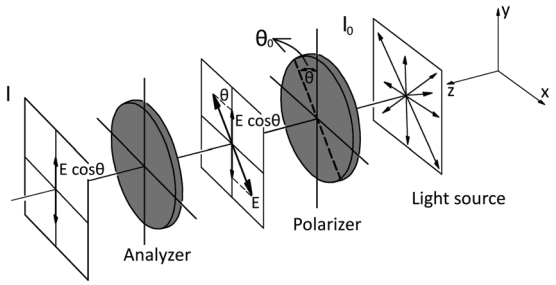

Fig. 1. Typical polarized light detecting system.

3. Displacement-current comparator

From Equation (1), we know that the relation between the light intensity I and the angular displacement θ is nonlinear. And light source drift is another contribution to the error of the optical system. To solve the problem of nonlinearity of the optical system effectively and eliminate the light source drift, a novel displacement sensor named a displacement-current comparator is presented [19].

3.1. Principle and configuration

The displacement-current is based on the polarized light detection principle and the Faraday optical rotation effect. As shown in Fig. 2, the system comprises a LED light source, a polarizer, a special analyzer, two diodes fixed on the other side of the analyzer and a Faraday rotator. The polarizer is coaxially mounted on a mechanical high precision linear displacement–angular displacement convertor which is used to convert the linear displacement to the angular displacement. The Faraday rotator consists of a solenoid and an optical active crystal. The special analyzer which is

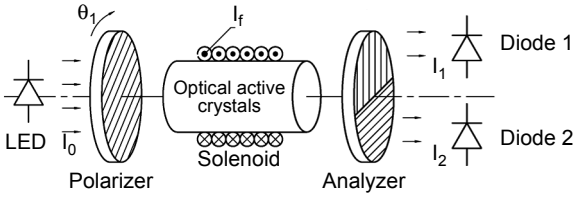

Fig. 2. Scheme of displacement-current comparator.

immobile consists of two polarizing discs which are fixed with their transmission axes perpendicular. The dual polarized light paths from one source are detected by two diodes respectively. I_1 and I_2 are light intensities detected by diode 1 and diode 2, respectively. When the sensor system is assembled, the initial angle of the transmission axes of the polarizer and the analyzer is adjusted to make sure that I_1 and I_2 are equal. When the angular displacement θ_1 is transmitted to the system, the intensity of magnetic field is regulated by controlling Faraday current to make sure that the light intensities I_1 and I_2 keep equal. When I_1 and I_2 are equal again, the value of the solenoid current is proportional to the input angular displacement θ_1. So, the sensor system measures the Faraday current I_f which is proportional to the input displacement, instead of measuring the displacement directly. The former is a simpler and more sophisticated task, in comparison to the latter. The essential theoretical derivation is given as follows.

According to Equation (1), we have:

$$I_1 = I_0 \cos^2(\theta_{01} + \theta_1 + \theta_2) \tag{3}$$

$$I_2 = I_0 \cos^2(\theta_{02} + \theta_1 + \theta_2) \tag{4}$$

Here, θ_{01} and θ_{02} are original angles between the transmission axis of the polarizer and the two polarizing discs mounted in the analyzer. I_1 and I_2 are light intensities detected by diode 1 and diode 2, respectively. Because the discrepancy between θ_{01} and θ_{02} is always 90°, the discrepancy between I_1 and I_2 can be expressed as follows:

$$\Delta I = I_1 - I_2 = -I_0 \sin\left[\theta_{01} + \theta_{02} + 2(\theta_1 + \theta_2)\right] \sin(\theta_{01} - \theta_{02}) \tag{5}$$

To eliminate the influence of light source intensity drift, we consider $\Delta I = 0$ which means $\theta_1 + \theta_2 = 0$ as the operation point of the system. And in order to get high sensitivity, we choose the operation point which can fit:

$$\left.\frac{\partial^2 \Delta I}{\partial(\theta_1 + \theta_2)^2}\right|_{\theta_1 + \theta_2} = 0$$

Then we can get the point: $\theta_{01} = \pi/4$, $\theta_{02} = 3\pi/4$.

From Equation (5), we know that $I_1 = I_2$ is true only if $\theta_{01} + \theta_{02} + 2(\theta_1 + \theta_2) = k\pi$ (wherein k is an integer). So, we can get

$$\theta_1 + \theta_2 = \frac{k\pi}{2} \tag{6}$$

From Equations (5) and (6), we know that the two output signals of photodiodes are equal if the polarization plane is rotated by the angle $\theta_2 = k\pi/2 - \theta_1$ by regulating Faraday current. Because I_1 and I_2 are from the same light source, the comparison relation of the two light intensities is independent of the light source drift, which means that the displacement information of the sensor system is resistant to the light source drift.

The relation between the Faraday current and the magnetic density can be expressed as follows:

$$B = a I_f \tag{7}$$

Here, a is the electromagnetic constant, and B is the magnetic density of the solenoid.

From Equations (2) and (7), we can get:

$$\theta_2 = \rho a L I_f \tag{8}$$

From Equations (6) and (8), we can get the value of the input angular displacement θ_1

$$\theta_1 = \frac{k\pi}{2} - \rho a L I_f \tag{9}$$

wherein, $-\pi/2 \le \rho a L I_f \le \pi/2$.

The current/displacement curve of the system is shown in Fig. 3. We can see that the linear relation between the Faraday current and the input displacement is periodic.

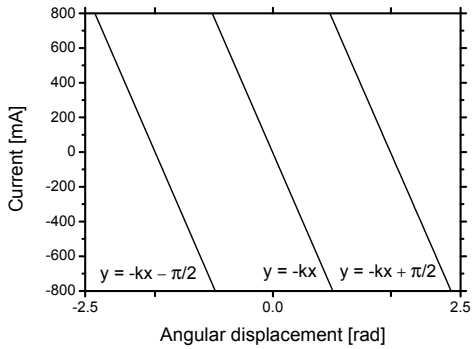

Fig. 3. Current/displacement curve of the sensor.

So, to realize wide range measurement, a secondary instrument should be used to record the order number of the period n. The finial output of the sensor can be expressed in the following way:

$$\theta_1 = -\rho a L I_f + \frac{n\pi}{2} \tag{10}$$

Otherwise, using the Faraday rotator with bigger length, higher Verdet constant and bigger electromagnetic constant is helpful for improving the sensor's sensitivity and range.

3.2. Experimental results

The linear–angular displacement convertor converts the input linear displacement X to the angular displacement θ_1 which brings the difference of the light intensities I_1 and I_2. The photoelectric convertors convert the light intensities to voltage values U_1 and U_2, and the voltage comparator gives the difference of U_1 and U_2. The current controller will regulate the Faraday current until the difference ΔU is eliminated; then, record the value of the Faraday current I_f and export it to the scope.

The experimental system of the sensor has been built to verify the concept. Figure 4**a** shows its schematic diagram. The system consists of a current modulator as the power supply, a stepping motor for generating regular displacement, a photoelectric encoder, a data acquisition card, a computer and the sensor system. The photoelectric encoder and the input axis of the sensor system are mounted coaxially.

Plastic polarizing discs are used as the polarizer, because of their low cost and high compactness. The plastic polarizing discs have different transmission coefficients to the lights with different wavelength, and have the best transmission coefficient to red light whose wavelength is 650–700 nm, so an infrared led is used as a light source. An intensity feedback control circuit is used to ensure the stability of the light source. The active crystal adopts the terbium glass whose Verdet constant is 0.34 min/Oe·cm corresponding to the light with the wavelength of 632.8 nm, and whose absorption coefficient is less than 0.5% per centimeter to the red light. The digital signal processing (DSP) adopts NI's product TMS320LF2407, whose A/D conversion digit number is 10. As the period of sensor system is $\pi/2$, the resolution of the sensor can

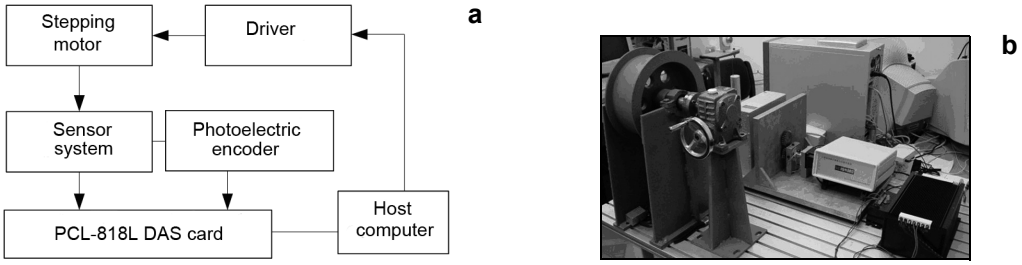

Fig. 4. Schematic of the experimental system (**a**), entity of the sensor and the experimental system (**b**).

be computed as this: $(\pi/2)/2^{10} = \pi/2048$. The referenced angular displacement is given by a photoelectric encoder whose resolution is 1/4024. The linear–angular displacement convertor consists of a high-accuracy wire spool convertor, a shrinker with constant force and a screw displacement compensator. The transmission ratio of the convertor is $180/\pi$ (mm/rad). So the linear revolution of the sensor system is $(\pi/2048)\times(180/\pi) =$ = 0.09 mm.

The entities of the prototype and the experimental system are shown in Fig. 4**b**. The experimental process is as follows: The detector is driven to rotate by an angular displacement θ by the stepping motor to simulate the wide range input displacement. The photoelectric encoder which is coaxially mounted on the detector gives the referenced value of the input displacement.

The results of the static measurement of multiperiod are shown in Fig. 5. After linearity fitting, we can get the performance parameter in the following way:

– Fitting curve: $y = 0.3519x$;
– Slope standard deviation: 3.16403×10^{-4};
– Correlation coefficients: 0.99999;
– Linearity fitting standard deviation: 1.18978.

Figure 5**b** shows the results of the dynamic measurement of multiperiod. Because the counter of PCL-818L is degressive, as the input displacement grows, the slope rate

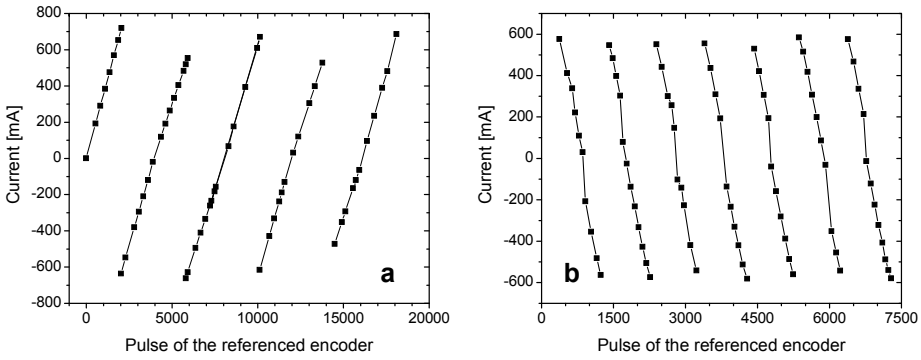

Fig. 5. Static measurement results of multiperiod (**a**), dynamic measurement results of multiperiod (**b**).

is negative. The linearity is ideal when the current is under or bellow zero, but there is a deviation when the current direction is reversing. The reason of the deviation is the calibration error of zero point of the PCL-818L. The periodic linearity of the curve is close to the periodic linearity of Fig. 5**b**. And after analyzing the data, we get: measuring range – 30 m, linearity – 0.002%, sensitivity – 1164.4 mA/rad, accuracy – $\leq \pm 0.3\%$.

3.3. Error analysis

From equation $\theta_1 = k\pi/2 - \rho a L I_f$, we know that the relationship between the rotation angle and the current is linear in one period, so the current measurement error is the direct contribution to the displacement measurement error. The current measurement error is up to 1‰.

The temperature drift of the Verdet constant which is up to 2‰ has a great influence on the systematic error. This error can be effectively reduced by the dynamic coefficient calibration when the sensor starts. And the temperature variation in the measurement process can be offset by temperature compensation. The length of the Faraday rotator and the value of the electromagnetic constant also bring systematic error.

The light intensities are converted into voltage signals U_1 and U_2 by the photoelectric diodes, so the equations (4) and (5) can be expressed as follows:

$$U_1 = k_1 I_0 \cos^2(\theta_{01} + \theta_1 + \theta_2) \tag{11}$$

$$U_2 = k_2 I_0 \cos^2(\theta_{02} + \theta_1 + \theta_2) \tag{12}$$

wherein, k_1 and k_2 are the coefficients of the two photoelectric circuits. In the initial moment, U_1 equals U_2. If the system (including the optical paths and the photoelectric circuits) is symmetric, the temperature drift of the circuits and variation of the light intensity will be offset, and no error will be generated. If the system is asymmetric, the asymmetry of the optical path and the circuits will bring error to the system.

We set:

$$f(\Delta U) = U_1 - U_2 = k_1 I_{01} \cos^2(\theta_{01} + \theta_1 + \theta_2) - k_2 I_{02} \cos^2(\theta_{02} + \theta_1 + \theta_2) \tag{13}$$

Clearly, the uniform light intensity in the projection spot of the LED has been adjusted by the pre-amplification circuit. Namely: $k_1 I_{01} = k_2 I_{02}$, the unevenness of the spot and inconsistent amplification of the circuits have been offset, and the light intensity difference is zero. But when the light source intensity drifts, different influence weights of light intensity variation for each point in the projection spot will lead to the variation of the detected light intensity, and the magnetic rotation misoperation will be caused. The light source has been pre-feedback, and the light stability error is within 5‰, so the error from this part is within 0.1‰. Similarly, the temperature drift of the circuit devices will cause the variation of the difference in the light intensity, and bring error to the system.

The digit capacity and the accuracy of the AD conversion circuit bring error too. The conversion error of the DSP TMS320LF2407 with 10-bit AD is 0.1‰. The relative error of the linear–angular displacement convertor is 0.148‰.

Plastic polarizing discs are used as the polarizer, and the transmission of the discs to the red light is >50%, and the extinction ratio is >100. The difference between the polarizing discs of the same type is tiny, so the error of this part can be omitted. The installation error between the planes of polarization of the sections of the analyzer is 0.1°, so the error of the installation is 0.1°/90° = 0.11%.

Through the analysis, it can be seen that the total error of the system is 0.23%. The other errors may come from the mechanical part.

4. Servo comparison displacement sensor

The displacement-current comparator solves the problems such as the nonlinearity, the light source intensity drift and the wide range measurement, but the temperature characteristic of the magneto-optically active material is not ideal, and the high price of magneto-optically active material will increase the cost of the sensor. To eliminate the disadvantage of the displacement-current comparator, a novel displacement sensor utilizing servo tracking technology is proposed.

4.1. Principle and configuration

The servo comparison displacement sensor utilizes a stepping motor to servo track the wide range input displacement. As shown in Fig. 6, the servo comparison sensor consists of a light source of LED, a polarizer, an analyzer with two polarizing disc rings mounted coaxially, two photoelectric detectors on the other side of the analyzer, and a stepping motor. There are three differences from the displacement-current

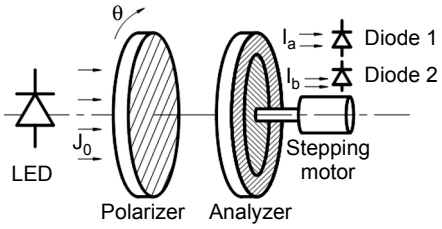

Fig. 6. Scheme of servo comparison displacement sensor.

comparator: *i*) The analyzer which is immobile in the displacement-current comparator can rotate with the stepping motor in the servo comparison displacement sensor; *ii*) The detector of the sensor system is simplified to decrease the cost; *iii*) The analyzer is different from the analyzer of the displacement-current comparator as shown in Fig. 6.

The linear input displacement X to be measured is converted to the angular displacement θ by a mechanical structure proportionally. The angular displacement θ_a is the angle between the transmission axis of the polarizer and the transmission

axis of the analyzer's inner ring. According to Malus law, θ_a has a certain relation with the light intensity I_a which is detected by the diode on the other side of the analyzer's inner ring

$$I_a = I_0 \cos^2(\theta_a) \tag{14}$$

wherein, I_0 is the light source intensity. And similarly, I_b which is the light intensity detected by the diode on the other side of the analyzer's outer ring can be expressed as follows:

$$I_b = I_0 \cos^2(\theta_b) \tag{15}$$

wherein θ_b is the angle between the transmission axis of the polarizer and the transmission axis of the analyzer's outer ring. To get the best linearity, θ_a is preset as $\pi/4$ and θ_b is preset as $3\pi/4$. The two discs are mounted orthogonally, and thus I_a is equal to I_b when there is no input displacement. When the linear displacement X is inputted continuously, the transmission axis of the polarizer will rotate by the angle θ which will make $I_a \neq I_b$. Then, the analyzer is driven by the step motor to turn a degree θ' to eliminate the difference in the two light intensities. Now, I_a and I_b can be expressed as follows:

$$I_a = I_0 \cos^2(\pi/4 + \theta - \theta') \tag{16}$$

$$I_b = I_0 \cos^2(3\pi/4 + \theta - \theta') \tag{17}$$

It can be seen that when $\theta = \theta'$, the equation $I_a = I_b$ is true, and *vice versa*. In other words, when the difference between two photoelectric signals from two respective light paths is zero, the turning angle driven by the step motor is equal to the turning angle caused by the input displacement. The number of control pulses of the step motor is an accurate value of the displacement being measured. In the dual light paths orthogonal differential comparison structure with the same light source, when the light intensity is drifting, the longitudinal coordinate of the preset working point (the point when the two photoelectric signals from the two respective light paths become equal) varies, but its transverse coordinate (the angular displacement) remains unchanged. That means that the system is resistant to light source intensity drift.

4.2. Experimental results

A prototype of the servo comparison sensor and its testing system are shown in Fig. 7**a**, and the entities are shown in Fig. 7**b**. A digital signal processing (DSP) chip is used as the control and output unit. Most components of the sensor are the same as the components of the displacement-current comparator. The three-phase hybrid stepping motor VRDM364/LHA and the driving system D921 of the Berger Lahr Company are used in this sensor. The pulses per rotating of the stepping motor

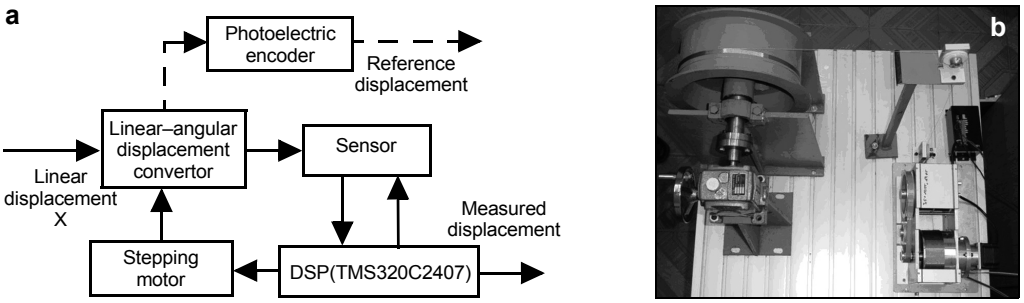

Fig. 7. Schematic diagram of the sensor and the test system (**a**), entity of the sensor and the test system (**b**).

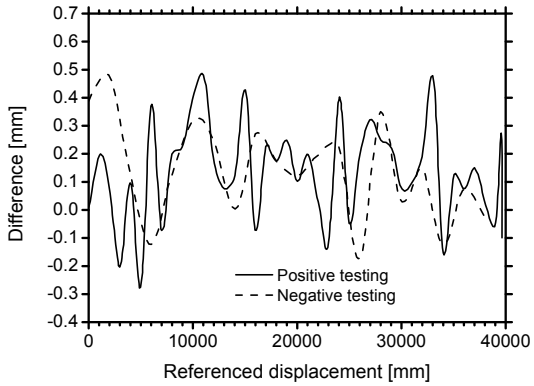

Fig. 8. Positive (**a**) and negative (**b**) testing results.

are 4000. The transmission ratio of the mechanical convertor is $180/\pi$ (mm/rad). So, the resolution of the sensor can be calculated as follows: $2\pi/4000 \times 180/\pi = 0.09$ mm.

Figure 8 shows the positive and negative testing results. The transverse coordinate of the curve is the referenced displacement value given by a photoelectric encoder with high accuracy. The testing results show that the performance parameter of the sensor is as follows. Measuring range: > 40 m; nonlinear error: 0.006%; repeatability error: ≤0.5 mm; accuracy: ≤±0.2%.

4.3. Error analysis

The servo comparison displacement sensor tracks the displacement directly to realize wide range measurement. The structure with one light source and dual light paths and the linear–angular displacement convertor are similar to the part of the current--displacement comparator, so the error analysis of polarizating discs and the convertor is the same as in Section 3.3, and the total error from this part is 0.12%.

We know $x = \pi\theta/2000$, wherein x is the measured displacement, θ is the measured angular displacement. In addition to the error brought by the optical path and photoelectric circuit asymmetry and AD conversion, the error caused by the losing

step and skipping step of the stepping motor is exiting in the serve comparison displacement sensor. The stepping motor and its driver of Berger Lahr Company can dynamically adjust the steps, pre-revolution-STEP. When STEP = 4000, losing step and skipping step of the motor do not happen. However, when STEP = 10000, phenomena of losing step and skipping step is obvious, and the experimental curve has jitters. So, the balance of the systematic error and sensitivity can be reached by setting a proper value of STEP, and the systematic error can be controlled effectively.

We can see that the properties of the sensor, such as speed, resolution, and accuracy, depend on the performance of the stepping motor. This may result in reduced lifespan or loss of accuracy of such sensor due to the wear of the motor. So, choosing a better stepping motor can effectively improve the performance of the sensor.

5. Conclusions

The research on wide range displacement sensors based on polarized light detecting technology has been carried out. A series of sensors are proposed. Several new structures, such as dual light paths with one light source, servo tracking technology, are introduced to the design of the sensors to eliminate optical nonlinearity, light source drift and to realize wide range measurement. The prototypes and the test beds have been fabricated, and the relevant testing results are given. The displacement-current comparator utilizes the Faraday rotation effect to convert the displacement to the current, and overcome the light source drift. The testing results of the prototype verify the concept very well, and show that the comparator has the linearity of 0.002%, and measuring range up to 30 m. But the comparator adopts magneto-optically active material whose temperature characteristic is not ideal, so a new kind of sensor named a servo comparison displacement sensor is proposed finally. The servo comparison displacement sensor abandons the active material, and utilizes the servo tracking technology to realize wide range measurement. The testing results of the prototype of the servo comparison displacement sensor show that the sensor has a nonlinearity error lower than 0.01% and measurement range up to 40 m.

Acknowledgements – This work was supported by the National Basic Research Program of China ("973" Program) 2007CB714000.

References

[1] LIU C., *Practical Sensors*, 3rd Ed., National Defense Industry Press, Bei Jing, 2004.

[2] GIRAO P.M.B.S., POSTOLACHE O.A., FARIA J.A.B., PEREIRA J.M.C.D., *An overview and a contribution to the optical measurement of linear displacement*, IEEE Sensors Journal **1**(4), 2001, pp. 322–331.

[3] KANOUN O., TRÄNKLER H.-R., *Sensor technology advances and future trends*, IEEE Transactions on Instrumentation and Measurement **53**(6), 2004, pp. 1497–1501.

[4] LU G., *Latest development of displacement measuring technology and its sensor*, World Manufacturing Engineering and Market **4**, 2005, pp. 72–73.

[5] BUSURIN V.I., SEMENOV A.S., UDALOV N.P., *Optical and fiber-optic sensors (review)*, Quantum Electronics **15**(5), 1985, pp. 595–621.

[6] KANOE M., TAKAHASHI G., SATO T., HIGAKI M., MORI E., OKUMURA K., *Optical voltage and current measuring system for electric power systems*, IEEE Transactions on Power Delivery **1**(1), 1986, pp. 91–97.
[7] RUDD R.E., III, MIDDLEBURY VT., *Polarizerless Magneto-Optic Speed and Torque Sensor*, USA Patent 5192862, 1993.
[8] XIANGYANG DENG, ZEREN LI, QIXIAN PENG, JUN LIU, JIANHUA TIAN, *Research on the magneto-optic current sensor for high-current pulses*, Review of Scientific Instruments **79**(8), 2008, p. 083106.
[9] DUNCAN W.M., CELII F.G., HENCK S.A., PARANJPE A.P., *Temperature Sensor and Method*, USA Patent 5501637, 1996.
[10] MORI H., ASAHARA Y., *Linearity of the Faraday-rotation-type ac magnetic-field sensor with a ferrimagnetic or ferromagnetic rotator film*, Applied Optics **35**(7), 1996, pp. 1083–1087.
[11] SAWA T., KUROSAWA K., KAMINISHI T., YOKOTA T., *Development of optical instrument transformers*, IEEE Transactions on Power Delivery **5**(2), 1990, pp. 884–891.
[12] PERCIANTE C.D., FERRARI J.A., *Faraday current sensor with temperature monitoring*, Applied Optics **44**(32), 2005, pp. 6910–6912.
[13] VILLAVERDE A.B., MUNIN E., PEDROSO C.B., *Linear displacement sensor based on the magneto--optical Faraday effect*, Sensors and Actuators A: Physical **70**(3), 1998, pp. 211–218.
[14] LI W., *Research on the principle and method of polarized light displacement sensor*, Chinese Journal of Scientific Instrument **20**(3), 1999, pp. 221–224.
[15] LI S., YANG C., ZHANG E., JIN G., *Compact optical roll-angle sensor with large measurement range and high sensitivity*, Optics Letters **30**(3), 2005, pp. 242–244.
[16] LI W., LU X., LIN Y., *Novel absolute displacement sensor with wide range based on Malus law*, Sensors **9**(12), 2009, pp. 10411–10422 (in Chinese).
[17] LIAO Y., LUO W., *A way of validating Malus law*, Physics Experimentation **21**(6), 2001, pp. 24–26 (in Chinese).
[18] AI Y., JIN Y., *Faraday magneto-optical rotation effect and its application*, Physics and Engineering **12**(5), 2002, pp. 50–60 (in Chinese).
[19] LI W., WANG Y., MA J., *Research on displacement-current comparator*, Journal of Zhejiang University **38**(7), 2004, pp. 860–863 (in Chinese).

Received June 7, 2010
in revised form September 12, 2010